available at www.sciencedirect.com

ScienceDirect

journal homepage: www.intl.elsevierhealth.com/journals/jden

Bone stress and interfacial sliding analysis of implant designs on an immediately loaded maxillary implant: A non-linear finite element study

Heng-Li Huang [a,*], *Jui-Ting Hsu* [a], *Lih-Jyh Fuh* [a], *Ming-Gene Tu* [a], *Ching-Chang Ko* [b], *Yen-Wen Shen* [c]

[a] *School of Dentistry, China Medical University, No. 91 Hsueh-Shih Road, Taichung 40402, Taiwan*
[b] *School of Dentistry, University of North Carolina at Chapel Hill, CB#7450, Chapel Hill, NC27599-7450, United States*
[c] *Dental Department, China Medical University Hospital, No2 Yu-Teh Road, Taichung 404, Taiwan*

ARTICLE INFO

Article history:
Received 17 July 2007
Received in revised form
21 February 2008
Accepted 21 February 2008

Keywords:
Immediately loaded implants
Implant designs
Sinus augmentation
CT-imaging
Finite element analysis

ABSTRACT

Objectives: This study investigated the surrounding bone stress and the implant–bone interfacial sliding of implant designs and implant sizes of immediately loaded implant with maxillary sinus augmentation by using three-dimensional (3D) non-linear finite element (FE) analysis.

Methods: Twenty-four FE models including four implant designs (cylindrical, threaded, stepped and step-thread implants) and three implant dimensions (standard, long and wide threaded implants) with a bonded and three levels of frictional contact of implant–bone interfaces were analyzed. The maxillary model was constructed from computer tomography (CT) images of a human skull and all 3D implant models were created via the computer-aided design (CAD) software.

Results: The use of threaded implants decreased the bone stress and sliding distance obviously about 30% as compared with non-threaded (cylindrical and stepped) implants. Increasing the implant's length or diameter reduced the bone stress by 13–26%. Employing a immediately loaded implant with smooth machine surface ($\mu = 0.3$, μ represents frictional coefficient) increased the bone stress by 28–63% as compared with the osseointegrated (bonded interfaces) implants. Roughening the implant surface ($\mu > 0.3$) did not reduced the bone stress, however it did decrease the interfacial sliding between implant and bone.

Conclusions: For an immediately loaded implant placed with sinus augmentation, using threaded implant could decrease both the bone stress and implant–bone sliding distance which may improve the implant initial stability and long-term survival. Rough surface of implants shows no benefit to reduce the bone stress but they could lower the interfacial sliding. On the contrary, employing long or wide implants decrease the bone stress but they cannot diminish the interfacial sliding.

* *Corresponding author*. Tel.: +1 886 4 22053366x2307; fax: +1 886 4 22014043.
E-mail address: hlhuang@mail.cmu.edu.tw (H.-L. Huang).

0300-5712/$ – see front matter
doi:10.1016/j.jdent.2008.02.015

1. Introduction

The delay loaded implant, which is covered by soft tissues and not subjected to loading for 4–6 months, has been used as the standard procedure of implant treatment. Dr. Brånemark[1] claimed that the ''4–6 months healing'' provided a stabilized bone-implant interface, called osseointegration that achieves high clinical success.[2,3] However, this delay-load concept has been challenged lately. The immediate loading (without the waiting period of healing time) has been proposed in contemporary dentistry to reduce the cost and time of the implant treatment.[4–6] Nevertheless, the effectiveness of an immediately loaded implant is unpredictable as compared to that of the delay loaded implant[5]. Some researchers found that the crestal bone loss and the failure rate of the immediately loaded implant were higher than that of delayed-loaded implant.[8–10] Conversely, Tarnow et al.[11] and Wallance et al.[12] both revealed no differences in the success rate between two treatment protocols; moreover, immediate loading might simulate crestal bone regeneration.[14,15]

Anatomic limitations such as the maxillary sinus cavity represent a challenge for the implant treatment in posterior maxilla. In order to increase the surrounding bony support of the implant the sinus grafted augmentation has been used clinically. However, high failure rate was documented in posterior maxilla for both the delay loaded implants[15] and the immediately loaded implants.[16]

Studies found that changing the implant size and the implant design could improve the outcome of the implant treatment. Employing longer or wider implants showed higher successful rates[13,17,18] and a better implant stability.[19] The use of threaded implants provided more engaging interface between implant and bone and improved the implant stability.[20] Additionally, the stepped shape of implant was suggested to create favorable load distribution due to its mimicking nature of the root form.[21] These advantages of the implant sizes and designs have been largely investigated in the delay loading treatment. However, for the immediate loading treatment the effects of these design parameters are still unknown especially in the cases with sinus grafted augmentation.

Modifying the implant surface by using micro-roughness techniques is recommended for implant treatment, because of the extended bone-implant contact area[22] and the stouter resistance for shear forces[20] by increasing surface friction. In addition, the surface-roughened implant has shown a lower failure rate than the machined implant.[23] Even thought the surface-roughened implants have been commonly used with sinus grafted augmentation, bone stress distribution of the immediately loaded implant is still unclear and remains to be determined.

The clinical predictability of the immediately loaded implant is primarily based on experiences rather than quantifiable evidence. Therefore, this study compared the biomechanical effects of the immediately loaded implant to the delay loaded (osseointegrated) implant under the considerations of sinus grafted augmentation with various implant designs, implants sizes, and roughed levels of implant surfaces. The finite element (FE) method of non-linear contact analysis is used for simulating the contact interfaces between the immediately loaded implant and bone.

2. Materials and methods

A serial of computer tomography (CT) images were selected from the premolar site to the second molar site of a dry human maxilla (Fig. 1a). From each CT image, material boundaries were delineated by an in-house imaging program ''CTTOOLS''. This program employs various thresholds in CT number and searches for maximum gradient values of the CT number, which can be used to detect the boundary pixels between different materials (Fig. 1b). A depth first search algorithm was then used to find the nearest boundary pixels and created the coordinates of points on the contour of each material. These coordinates were then input into the computer-aided design (CAD) software of SolidWorks (SolidWorks, SolidWorks Corp., Concord, MA, USA) to generate a 3D solid model of the posterior maxilla.

An implant-retained crown made of resin was duplicated from the first molar to create a serious of CT images. These CT images were then used to produce a 3D solid model of a crown by the same procedure mentioned above. The implant models were constructed by CAD software of SolidWorks. For the precise threaded characteristics, the helical sweep functions were utilized to create a spiral v-shape thread (Fig. 2). All models were combined by Boolean operations, the IGES format of the solid model was then imported into ANSYS Workbench (Swanson Analysis Inc., Huston, PA, USA) to generate the FE model (Fig. 3) by using 10-node tetrahedral h-elements (ANSYS solid 187).

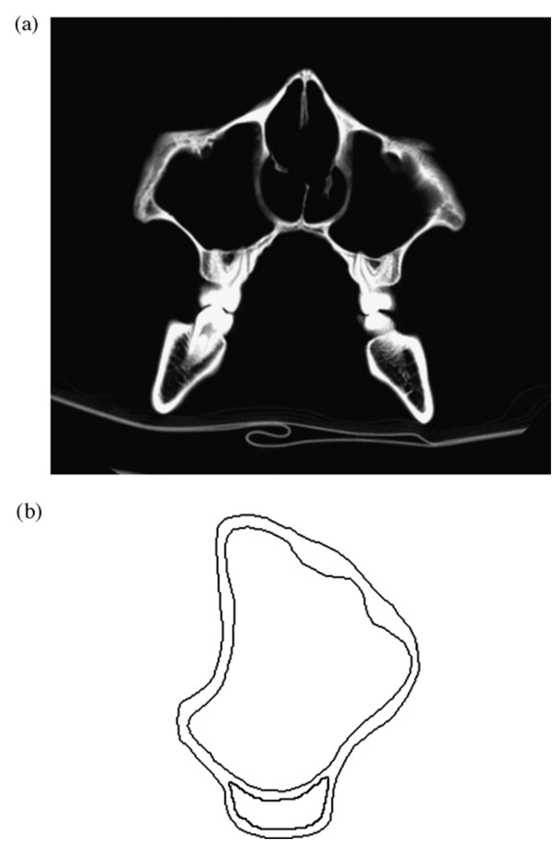

Fig. 1 – The interval distance between (a) CT images was 1 mm. (b) Contours of cortical bone, trabecular bone and sinus cavity.

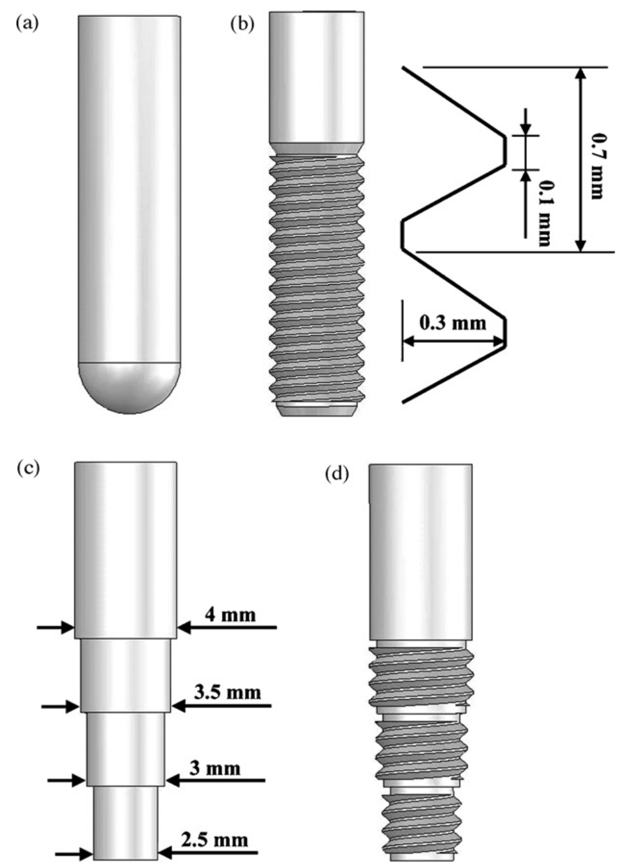

Fig. 2 – The solid models of (a) the cylindrical implant, (b) the thread implant, (c) the stepped implant and (d) the step-thread implant.

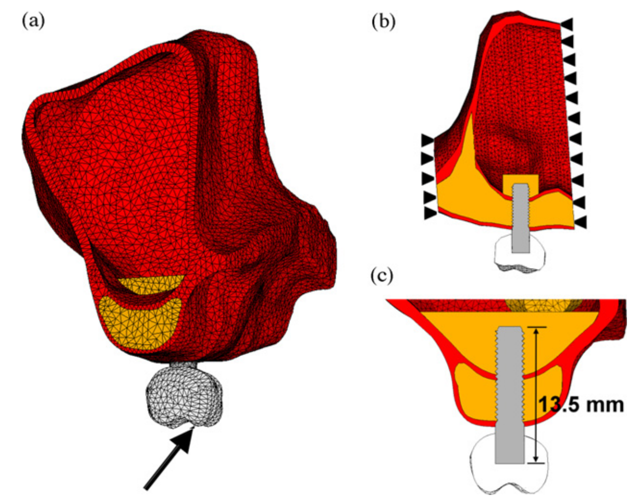

Fig. 3 – (a) The finite element model including the crown, the implant, the posterior maxilla and the grafted bone. A 129 N of oblique load with 30° was applied to the lingual cusp of the crown. (b) The mesial–distal and (c) buccal–lingual cross-sections of model were revealed. The boundary condition was set to fix the buccal and lingual surfaces of the maxillary bone.

Twenty-four FE models included six implants (a cylindrical implant, a threaded implant, a stepped implant, a step-thread implant, a long-length of threaded implant and a wide-diameter of threaded implant) with four conditions of implant–bone interfaces (0.3, 0.45 and 1.0 of frictional contact interfaces and a bonded interface) were constructed in this study. In order to discriminate these models easily, three sets of symbols were used. The first symbol denotes the implant size: "S" for the standard size of implant (11.5 mm in implant length and 4 mm in implant diameter); likewise "L" and "W" symbolized the longer (13.5 mm in implant length) and the wider implant (5 mm in implant diameter), respectively. The second symbol represented implant design (Fig. 2): "Cylinder" for the cylindrical implant, "Thread" for the threaded implant, "Step" for the stepped implant and "StepThread" for the stepped-thread implant. The third symbol indicated the implant–bone interface conditions: "F0.3" for $\mu = 0.3$ of the interfaces between a smooth metal surface and bone[24] (μ represents frictional coefficient), "F0.45" for $\mu = 0.45$ of the interfaces of the interfaces between a porous metal surface and bone,[24] "F1" for $\mu = 1$ of the interfaces between the excessive roughness of metal surface and bone, and "Bond" for bonded interface between metal and bone. For simulating the slide and stick of the frictional contact behavior, non-linear surface-to-surface contact elements (ANSYS conta 174 and targe 170) were adopted in the models. The dimensions of the maxillary model are about 30.3 mm long (mesiodistal), 16.3 mm height at the premolar site, 45.4 mm height at the second molar site, 5.4 mm width (buccolingual) at the crestal bone of the premolar site, and 10.1 mm width (buccolingual) at the crestal bone of the second molar site.

The material properties of implant, prosthetic crown, maxilla and grafted bone (Table 1) were assumed to be isotropic and linearly elastic.[25,26] The 129 N of the buccal oblique force[27] was applied with 30° to the long axis of the implant on the buccal cusp (Fig. 3a). The mesial and distal surfaces of maxillary bone were constrained in x, y and z directions (displacements = 0) as the boundary condition (Fig. 3b). In FE analysis, the outcome is only approximate rather than the exact solution. Therefore, the convergence test of the FE models was performed to verify the mesh quality, and the convergence criterion was set to be less than 6% changes of the highest von-Mises stress of bone between the element sizes. Based on the result of the convergent test, therefore, 0.7 mm of element size was utilized as the meshing requirement for all FE models. Fig. 4 shows the process of convergent test of Model S-Thread-Bond as an example.

Table 1 – Materials properties used in FE mode

Material	Young's modulus, E (MPa)	Poisson's ratio, ν
Cortical bone	13,800	0.26
Trabecular bone	345	0.31
Titanium	110,000	0.35
Porcelain	70,000	0.19
Grafted bone	345	0.31

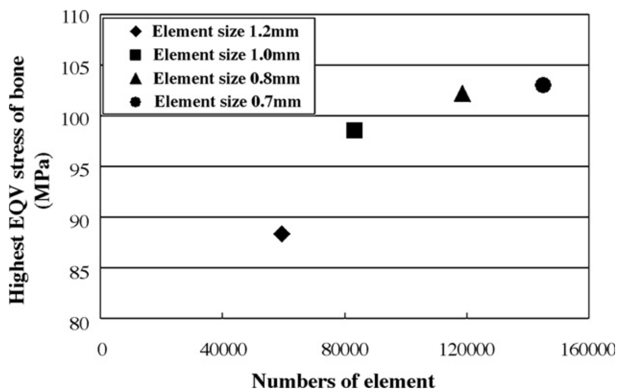

Fig. 4 – The convergence test of FE models, which were meshed by 1.2 mm, 1.0 mm, 0.8 mm and 0.7 mm of element sizes.

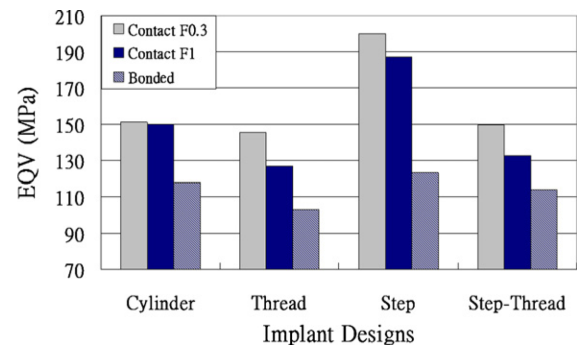

Fig. 5 – The comparison of the maximum von-Mises stress (EQV) in bone among four implant designs with bonded and contact (μ = 0.3 and 1, μ represents the frictional coefficient) of implant–bone interfacial statuses.

3. Results

Comparison of six implant designs for osseointegrated implants (bonded interfaces), stepped implant and cylindrical implant showed higher von-Mises (EQV) stresses than other implants designs (Table 2, Fig. 5). However, adding a threaded characteristic into the stepped implant and cylindrical implant decreased the bone stress by 13% in Model S-Thread-Bond and 8% in Model S-Step-thread-Bond as contrasted with Model S-Cylinder-Bond and Model S-Step-Bond, respectively. The use of the longer implant did not reduce the bone stress; however, enlarging implant's diameter diminished the bone stress by 16% in Model W-Thread-Bond as compared with Model S-Thread-Bond (Table 2, Fig. 6).

The models assumed the contact interface between a smooth metal surface and bone (μ = 0.3) increased 28–63% of the bone stress (EQV) obviously as compared with that on bonded interfaces. Also, in general the small stress diminution of bone were observed in the porous surface of implant (μ = 0.45) or the excessive rough surface of implant (μ = 1) than that of a smooth surface of implant (μ = 0.3).

Comparison of six implant designs for immediately loaded implants (contact interfaces), stepped implant showed the highest bone stress (Table 2, Fig. 5). The use of threaded implant decreased bone stress by 4% in Model S-Thread-F0.3, 11% in Model S-Thread-F0.45 and 15% Model S-Thread-F1 as contrasted with Model S-Cylinder-F0.3, Model S-Cylinder-F0.45 and Model S-Cylinder-F1, respectively. Likewise, adding threaded characteristic into the stepped implant body reduced the bone stress by 20% in Model S-Stepthread-F0.3, 26% in Model S-Stepthread-F0.45 and 30% in Model S-Stepthread-F1 as compared with Model S-Stepr-F0.3, Model S-Step-F0.45 and Model S-Step-F1, respectively. As contrasted with standard size of threaded implant (Table 2, Fig. 6), when increasing implant's length the bone stress (EQV) were lowered by 18%

Table 2 – The maximum von-Mises stress (EQV), the peak maximum principal stress (S1) and the peak minimum principal stress (S2) of the cortical bone around different design of implant with various bone–implant interface conditions

Interface	Implant	EQV (MPa)	S1 (MPa)	S2 (MPa)
Bonded	Cylinder	118.0	61.3	−153.9
	Thread	103.0	74.0	−136.3
	Step	123.4	112.5	−158.6
	Step-thread	113.9	74.0	−136.3
	Thread (long)	102.4	72.8	−130.0
	Thread (wide)	88.0	48.2	−113.0
Contact (F0.3)	Cylinder	151.0	57.2	−147.3
	Thread	145.5	48.6	−160.0
	Step	200.0	86.9	−200.6
	Step-thread	149.5	52.9	−163.9
	Thread (long)	119.5	43.7	−143.4
	Thread (wide)	107.1	30.8	−119.6
Contact (F0.45)	Cylinder	157.5	55.8	−189.8
	Thread	140.5	55.5	−161.8
	Step	195.5	97.0	−233.9
	Step-thread	145.5	55.3	−172.6
	Thread (long)	115.5	51.0	−141.3
	Thread (wide)	103.5	28.4	−123.3
Contact (F1)	Cylinder	150.3	75.0	−191.8
	Thread	127.0	75.8	−152.9
	Step	187.3	125.7	−197.1
	Step-thread	132.4	76.5	−153.8
	Thread (long)	111.5	70.2	−135.0
	Thread (wide)	95.8	40	−118.1

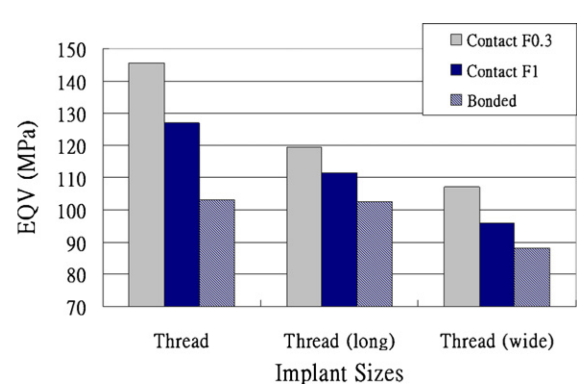

Fig. 6 – The comparison of the Maximum von-Mises stress (EQV) in bone among three implant sizes with bonded and contact (μ = 0.3 and 1) of implant–bone interfacial statuses.

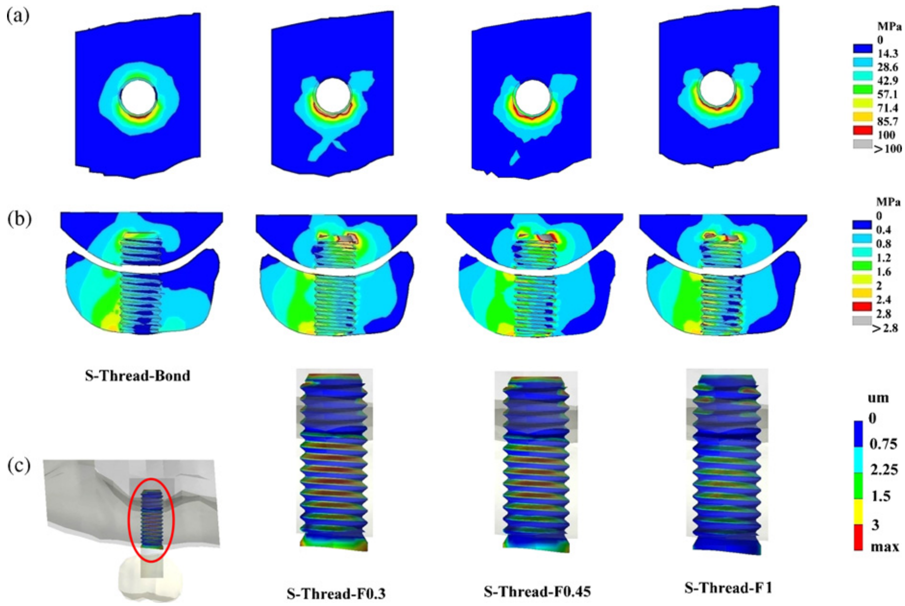

Fig. 7 – The distribution of (a) cortical bone stresses, (b) trabecular and grafted bone stresses and (c) interfacial sliding distances between implant and bone among a bonded and three contact models.

in L-Thread-F0.3, 22% in L-Thread-F0.45 and 13% in L-Thread-F1; similarly when implants were widened the bone stress were diminished by 26% in W-Thread-F0.3, 26% in W-Thread-F0.45 and 24% in W-Thread-F1.

The von-Mises stress distributions of cortical bone (Figs. 7–9) showed that the high stresses were located at the crestal region around the implant, which corresponded with the clinical finding of maxillary crestal bone loss.[28] As compared with the models of bonded implant–bone interface, the models of smooth metal surface ($\mu = 0.3$) extended the areas of high stresses in crestal cortical bone and in the bone regions near the apex of implant and the stepped areas where the implant's diameter changes in the stepped implant (Figs. 7 and 8). However, for the threaded implants increasing the frictional coefficient at implant–bone interfaces seems to direct the stresses away from high stress regions and transferred them into the bone areas near the tip of the threads (Fig. 7).

On the comparison of the highest maximum principal (tensile) stresses and highest minimum principal (compressive) stresses between bonded and contact implant–bone interfaces (Table 2), the models of contact interfaces ($\mu = 0.3$, 0.45 and 1) shows higher compressive stresses of bone than that on bonded interfaces. Enlarging the value of frictional coefficient shows no significant influence for increasing or decreasing the tensile and compressive stresses of bone.

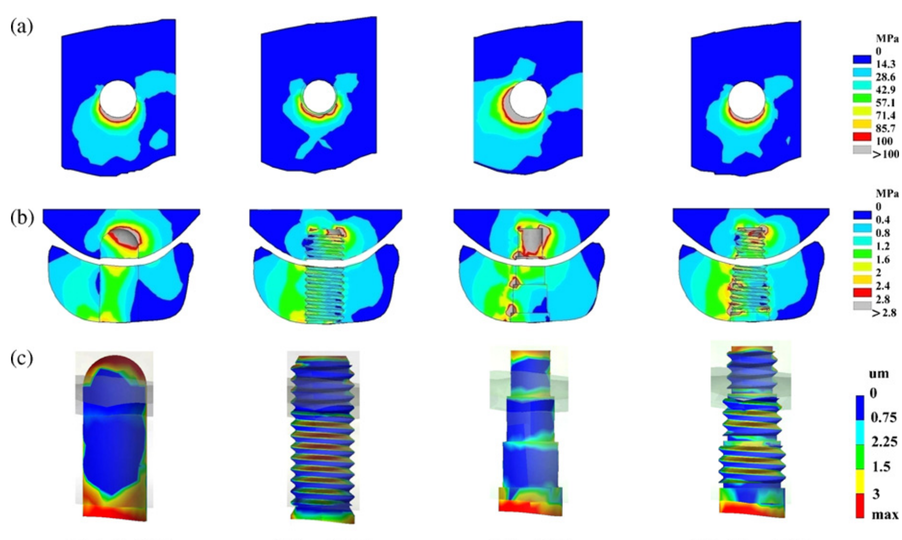

Fig. 8 – The distribution of (a) cortical bone stresses, (b) trabecular and grafted bone stresses and (c) interfacial sliding distances between the implant and bone among four implant designs.

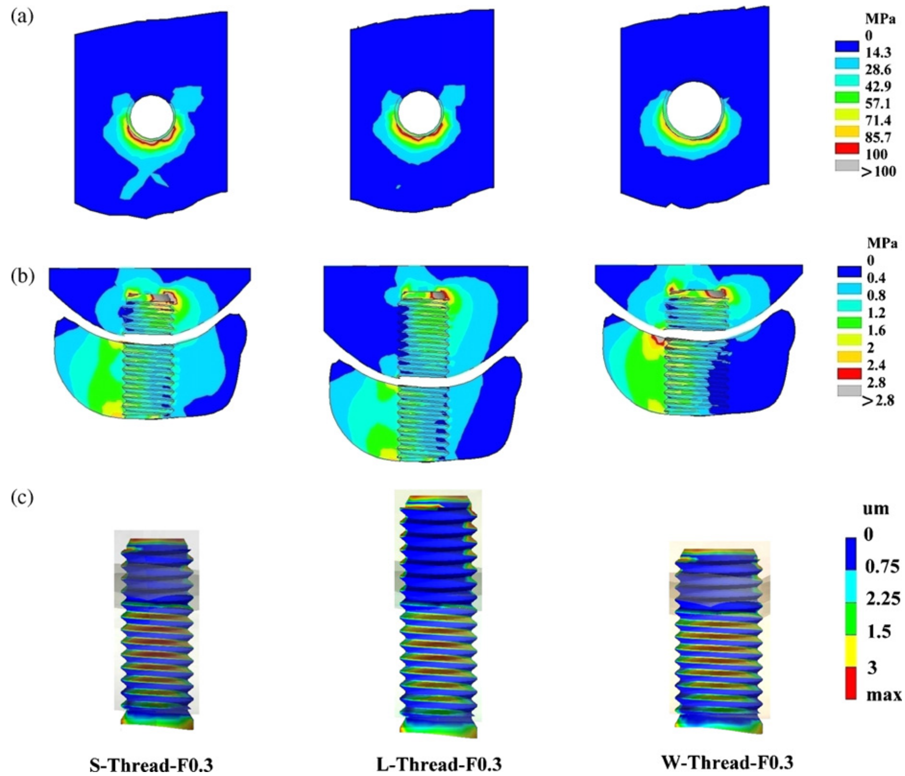

Fig. 9 – The distribution of (a) cortical bone stresses, (b) trabecular and grafted bone stresses and (c) interfacial sliding distances between the implant and bone among three implant sizes.

The maximum sliding distances between the implant and bone were located at the crestal region, the apex of implant and the thread near the apex of implant (Table 3). Increasing the frictional coefficient of the interfaces from 0.3 to 1, the interfacial sliding between implant and bone was mainly reduced from 20% to 30–60% (Table 3 and Fig. 7). For the machine surface of implant ($\mu = 0.3$), the stepped design revealed a largest sliding distance among six models. Using characteristic of thread on implant surface could reduce the implant–bone interfacial sliding (Table 3 and Fig. 8). Threaded design of implants decreased the sliding distance by 41% in Model S-Thread-F0.3 and 35% in Model S-Stepthread-F0.3 as compared with Model S-Cylinder-F0.3 and Model S-Step-F0.3 respectively. No significant difference was shown in the sliding value and sliding distribution (Table 3 and Fig. 9) of the standard size of implant (Model S-Thread-F0.3), the long length of implant (Model L-Thread-F0.3) and the wide diameter of implant (Model W-Thread-F0.3).

Table 3 – The maximum sliding distance (μm) of model of contact implant–bone interfaces and it's location

Interface	Implant	μm	Location
Contact (F0.3)	Cylinder	21.3	I
	Thread	12.5	II
	Step	20.0	I
	Step-thread	13.1	I
	Thread (long)	10.8	II
	Thread (wide)	13.0	III
Contact (F0.45)	Cylinder	13.2	II
	Thread	10.1	II
	Step	15.7	II
	Step-thread	10.1	II
	Thread (long)	8.7	II
	Thread (wide)	12.3	III
Contact (F1)	Cylinder	8.6	II
	Thread	8.4	III
	Step	8.2	II
	Step-thread	5.5	II
	Thread (long)	7.8	III
	Thread (wide)	8.6	III

The locations I, II and III indicate the crestal region, the apex of implant and the thread near the apex of implant.

4. Discussion

To date, there is no general consensus for the use of the immediately loaded implant especially in posterior maxilla with sinus augmentation. Applying engineering analyses may provide a useful prediction in the implant design. Following the previous simplified models,[29,30] the present study mimicked actual maxillary sinus and the associated implants using three-dimensional CAD technologies, boundary detecting program for CT images and the non-linear FE contact analysis. It might provide the clues to interpret the biomechanical effect of the clinical use of the implants (included cylindrical, threaded and stepped designs) as well as the implant surface roughness (included $\mu = 0.3$ for smooth implant surface and $\mu > 0.3$ for rough implant surface; μ represents frictional coefficient) for the immediately loaded maxillary implant.

Employing stepped design into the implant body did not decrease the stress of bone among six models; however, adding threaded characteristic into the implant body did. The stepped implant is proposed for its root-form shape, which is speculated about favorable stress dissipation at surrounding bone. Nevertheless, in our results employing the stepped design into the implant body did not reduce the bone stress because the stepped design diminishes the diameter of implant, which also decreases the contact area between the implant and bone. From the mechanical standpoint, the reduction of contact areas raised the stress at the surrounding bone as compared with the cylindrical implant. However, adding the threaded characteristic to the implant, which increased implant surface areas,[7] showed an advantage by decreasing the peak stress for both osseointegrated and immediate loading cases. In addition, the threaded design could resist sliding at the interface even though the frictional coefficient was low ($\mu = 0.3$) in the immediately loaded implant. Based on the results, it is recommended to use threaded design to achieve favorable bone stress and initial stability, especially for immediate loading cases.

This study showed that placing a long osseointegrated implant in maxilla did not significantly decrease the bone stress. However, increasing the implant length for the immediately loading treatment did lower the peak bone stress. For a delay loading treatment, our result was consistent with that of previous studies[31] and showed that most of the stresses are concentrated at the crestal cortical bone. Therefore, increasing the implant's length does not decrease the peak bone stresses because the load bearing area (interfaces) between implant and cortical region is a constant (no increase). Nevertheless, for an immediately loaded implant, stress dissipation depended on the amount of the implant surface contacting with bone during the loading. It is interesting to note that the circumferential contact interfaces at the crestal cortical region of the long implant (13.5 mm) was larger than that of the short implant. Furthermore, widening the implant's diameter showed a reduction in the bone stresses at both delay loading and immediate loading treatments due to the enlarged bone-implant contact area[26] and the diminution of the bending effect by decreasing the ratio of crown and implant lengths.[18] According to the results of the present study, the increase of the implant's length and diameter could be proposed for single tooth restorations of immediately loaded maxillary implant.

Compared with the bonded interfaces (osseointegrated implant), the low frictional coefficient of contact interface (immediately loaded implant) yielded higher stresses in cortical bone. This result agreed (Figs. 5 and 6) with the outcome of Van Oosterwyck et al.[32] Through the bonded interface the force was dissipated evenly in both the compressive site and the tension site. However, on the contact interfaces force was not transferred through the tension site. Therefore, force only passed through the compressive site, which resulted in excessive stresses. These disproportionately high and low stresses may result in a high risk of surrounding bone loss[28] due to disuse atrophy[33] or overloading resorption. However, in this study we did not signify that the possibility of surrounding bone loss induced by these inappropriate bone stresses would increase the implant failures. For immediately loaded implant, the effect of initial implant stability is also essential. Brunski et al.[34] suggested the micromotion between the implant and bone needed to be less than 100 μm in order to develop an osseointegrated interface instead of fibrous encapsulation. In our models assuming there was no gap at bone-implant interfaces before loading, the results demonstrated that the maximum sliding distance of the contact interfaces ($\mu = 0.3$, 0.45 and 1) was less than one fifth of this critical value (100 μm). The finding of this investigation might explain why several reports have shown that the use of the immediate loading treatment still could lead to the osseointegration[35] and showed no significant difference in survival rate with using delay loading treatment.[28,36] A higher frictional coefficient of implant–bone interface did not reduce the peak stresses at surrounding bone extensively. However, increasing the value of frictional coefficient of interface did decrease the micromotion at bone-implant interfaces. That might be beneficial to increase the implant stability and survival rates.[23,36]

Limitations of this study are (1) simplified homogeneous, isotropic material properties used and (2) frictional coefficient of roughed implant. To the best of our knowledge, all anisotropic bone properties were measured from mandible. Parametrically altering maxillary properties with anisotropic assumption may result in different stress patterns; this requires further studies such as the measurement of anisotropic properties by compressive testing[37] and ultrasonic velocities[38] or inhomogeneous properties from CT Images[39] Otherwise, although the effects of frictional coefficient of porous implant have been discussed in the study, the effect of the frictional coefficient of the current use of rough implants has not been evaluated. It needs to be considered in the further investigation.

5. Conclusion

Within the limitations of this study, the following conclusions for an immediately loaded maxillary implant are suggested:

1. Around the immediately loaded implant (contact bone-implant interfaces), the peak bone stress is higher than that around the osseointegrated implant (bonded interfaces).
2. The maximum sliding distance of the contact interfaces of models is lower than 100 μm, which might explain the clinical observation that employing the immediate loading treatment can lead to osseointegration.
3. For immediate loading treatment, adding a threaded characteristic into implant shows an ability to decrease both the bone stress and the sliding distance. Increasing frictional coefficient of implant–bone interfaces does not lower the bone stress significantly, but reduces the interfacial sliding distance. These benefits might diminish the risk of implant failure.
4. Increase the implant's length does not decrease the bone stress of osseointegrated implant. However, it does reduce the bone stress of immediately loaded implant. Widening

the implant's diameter decreases the bone stress at both delay and immediately loaded implant.

Acknowledgement

This research was supported by China Medical University (CMU96-143), Taiwan.

REFERENCES

1. Brånemark PI, Hansson BO, Adell R, Rieine U, Lindström J, Hallén O, Ohman A. Osseointegrated implants in the treatment of the edentulous jaw. Experience from a 10-year period. *Scandinavian plastic and reconstructive surgery* 1977;**16**:131–2.
2. Adell R, Lekholm U, Rockler B, Brånemark PI. A 15-year study of osseointegrated implants in the treatment of edentulous jaw. *International Journal of Oral Surgery* 1981;**10**:387–416.
3. van Steenberghe D, Lekholm U, Bolender C, Folmer T, Henry P, Herrmann I. The application of osseointegrated oral implants in the rehabilitation of partial edentulism: a prospective multicenter study on 558 fixtures. *The International Journal of Oral and Maxillofacial Implants* 1990;**5**:272–82.
4. Szmukler-Moncler S, Piattelli A, Favero GA, Dubruille JH. Considerations preliminary to the application of early and immediate loading protocols in dental implantology. *Clinical Oral Implants Research* 2000;**11**:12–25.
5. Misch CE, Wang HL, Misch CM, Sharawy M, Lemons J, Judy KW. Rationale for the application of immediate load in implant dentistry: Part I. *Implant Dentistry* 2004;**13**:207–17.
6. Misch CE, Wang HL, Misch CM, Sharawy M, Lemons J, Judy KW. Rationale for the application of immediate load in implant dentistry: Part II. *Implant Dentistry* 2004;**13**: 310–21.
7. Gapski R, Wang HL, Mascarenhas P, Lang NP. Critical review of immediate implant loading. *Clinical Oral Implants Research* 2003;**14**:515–27.
8. Sagara M, Akagawa Y, Nikai H, Tsuru H. The effects of early occlusal loading on one-stage titanium alloy implants in beagle dogs: a pilot study. *The Journal of Prosthetic Dentistry* 1993;**69**:281–8.
9. Schnitman PA, Wohrle PS, Rubenstein JE, DaSilva JD, Wang NH. Ten-year results for Branemark implants immediately loaded with fixed prostheses at implant placement. *The International Journal of Oral and Maxillofacial Implants* 1997;**12**:495–503.
10. Balshi TJ, Wolfinger GJ. Immediate loading of Branemark implants in edentulous mandibles: a preliminary report. *Implant Dentistry* 1997;**6**:83–8.
11. Tarnow DP, Emtiaz S, Classi A. Immediate loading of threaded implants at stage 1 surgery in edentulous arches: ten consecutive case reports with 1- to 5-year data. *The International Journal of Oral and Maxillofacial Implants* 1997;**12**:319–24.
12. Wallace SS, Froum SJ. Effect of maxillary sinus augmentation on the survival of endosseous dental implants. A systematic review. *Annals of Periodontology/The American Academy of Periodontology* 2003;**8**:328–43.
13. Randow K, Ericsson I, Nilner K, Petersson A, Glantz PO. Immediate functional loading of Branemark dental implants. An 18-month clinical follow-up study. *Clinical Oral Implants Research* 1999;**10**:8–15.
14. Ko CC, Swift JQ, DeLong R, Douglas WH, Kim YI, An KN, Chang CH, Huang HL. An intra-oral hydraulic system for controlled loading of dental implants. *Journal of Biomechanics* 2002;**35**:863–9.
15. Buser D, Mericske-Stern R, Bernard JP, Behneke A, Behneke N, Hirt HP, Belser UC, Lang NP. Long-term evaluation of non-submerged ITI implants. Part 1: 8-year life table analysis of a prospective multi-center study with 2359 implants. *Clinical Oral Implants Research* 1997;**8**:161–72.
16. Glauser R, Ree A, Lundgren A, Gottlow J, Hammerle CH, Scharer P. Immediate occlusal loading of Branemark implants applied in various jawbone regions: a prospective. 1-Year clinical study. *Clinical Implant Dentistry and Related Research* 2001;**3**:204–13.
17. Blomqvist JE, Alberius P, Isaksson S. Two-stage maxillary sinus reconstruction with endosseous implants: a prospective study. *The International Journal of Oral and Maxillofacial Implants* 1998;**13**:758–66.
18. Davarpanah M, Martines H, Kebir M, Etienne D, Tecucianu JF. Wide-diameter implants: new concepts. *The International Journal of Periodontics Restorative Dentistry* 2001;**21**: 149–59.
19. Ochi S, Morris HF, Winkler S. The influence of implant type, material, coating, diameter, and length on periotest values at second-stage surgery: DICRG interim report no. 4. Dental Implant Clinical Research Group. *Implant Dentistry* 1994;**3**:159–62.
20. Sykaras R, Iacopino AM, Marker VA, Triplett RG, Woody RD. Implant materials, designs, and surface topographies: their effect on osseointegration. A literature review. *The International Journal of Oral and Maxillofacial Implants* 2000;**15**:675–90.
21. Maiorana C, Santoro F. Maxillary and mandibular bone reconstruction with hip grafts and implants using Frialit-2 implants. *The International Journal of Periodontics Restorative Dentistry* 2002;**22**:221–9.
22. Buser D, Schenk RK, Steinemann S, Fiorellini JP, Fox CH, Stich H. Influence of surface characteristics on bone integration of titanium implants. A histomorphometric study in miniature pigs. *Journal of Biomedical Materials Research* 1991;**25**:889–902.
23. Wagenberg B, Froum SJ. A retrospective study of 1925 consecutively placed immediate implants from 1988 to 2004. *The International Journal of Oral and Maxillofacial Implants* 2006;**21**:71–80.
24. Rancourt D, Shirazi-Adl A, Drouin G, Paiement G. Friction properties of the interface between porous-surfaced metals and tibial cancellous bone. *Journal of Biomedical Materials Research* 1990;**24**:1503–19.
25. Rees JS, Hammadeh M. Undermining of enamel as a mechanism of abfraction lesion formation: a finite element study. *European Journal of Oral Sciences* 2004;**112**:347–52.
26. Huang HL, Huang JS, Ko CC, Hsu JT, Chang CH, Chen MY. Effects of splinted prosthesis supported a wide implant or two implants: a three-dimensional finite element analysis. *Clinical Oral Implants Research* 2005;**16**:466–72.
27. Morneburg TR, Proschel PA. Measurement of masticatory forces and implant loads: a methodologic clinical study. *The International Journal of Prosthodontics* 2002;**15**:20–7.
28. Herzberg R, Dolev E, Schwartz-Arad D. Implant marginal bone loss in maxillary sinus grafts. *The International Journal of Oral and Maxillofacial Implants* 2006;**21**:103–10.
29. Fanuscu MI, Iida K, Caputo AA, Nishimura RD. Load transfer by an implant in a sinus-grafted maxillary model. *The International Journal of Oral and Maxillofacial Implants* 2003;**18**:667–74.
30. Koca OL, Eskitascioglu G, Usumez A. Three-dimensional finite-element analysis of functional stresses in different bone locations produced by implants placed in the

maxillary posterior region of the sinus floor. *Journal of Prosthetic Dentistry* 2005;**93**:38–44.
31. Tada S, Stegaroiu R, Kitamura E, Miyakawa O, Kusakari H. Influence of implant design and bone quality on stress/strain distribution in bone around implants: a 3-dimensional finite element analysis. *The International Journal of Oral and Maxillofacial Implants* 2003;**18**:357–68.
32. Van Oosterwyck H, Duyck J, Vander Sloten J, Van der Perre G, De Cooman M, Lievens S, Puers R, Naert I. The influence of bone mechanical properties and implant fixation upon bone loading around oral implants. *Clinical Oral Implants Research* 1998;**9**:407–18.
33. Cehreli M, Sahin S, Akca K. Role of mechanical environment and implant design on bone tissue differentiation: current knowledge and future contexts. *Journal of Dentistry* 2004;**32**:123–32.
34. Brunski JB, Puleo DA, Nanci A. Biomaterials and biomechanics of oral and maxillofacial implants: current status and future developments. *The International Journal of Oral and Maxillofacial Implants* 2000;**15**:15–46.
35. Degidi M, Scarano A, Iezzi G, Piattelli A. Periimplant bone in immediately loaded titanium implants: histologic and histomorphometric evaluation in human. A report of two cases. *Clinical Implant Dentistry and Related Research* 2003;**5**:170–5.
36. Del Fabbro M, Testori T, Francetti L, Weinstein R. Systematic review of survival rates for implants placed in the grafted maxillary sinus. *The International Journal of Periodontics and Restorative Dentistry* 2004;**24**:565–77.
37. O'Mahony AM, Williams JL, Katz JO, Spencer P. Anisotropic elastic properties of cancellous bone from a human edentulous mandible. *Clinical Oral Implants Research* 2000;**11**:415–21.
38. Schwartz-Dabney CL, Dechow PC. Variations in cortical material properties throughout the human dentate mandible. *American Journal of Physical Anthropology* 2003;**120**:252–77.
39. Zhang F, Peck CC, Hannam AG. Mass properties of the human mandible. *Journal of Biomechanics* 2002;**35**:975–8.